Developmental Biology 433 (2018) 448–460

Contents lists available at ScienceDirect

Developmental Biology

journal homepage: www.elsevier.com/locate/developmentalbiology

Original research article

Organ specific gene expression in the regenerating tail of *Macrostomum lignano*

Birgit Lengerer[a], Julia Wunderer[a], Robert Pjeta[a], Giada Carta[c], Damian Kao[b], Aziz Aboobaker[b], Christian Beisel[d], Eugene Berezikov[e], Willi Salvenmoser[a], Peter Ladurner[a,*]

[a] Institute of Zoology and Center of Molecular Bioscience Innsbruck, University of Innsbruck, Technikerstr. 25, A-6020 Innsbruck, Austria
[b] Department of Zoology, University of Oxford, South Parks Road, Oxford OX1 3PS, United Kingdom
[c] Division of Physiology, Medical University of Innsbruck, Schöpfstraße 41/EG, A-6020 Innsbruck, Austria
[d] Department of Biosystems Science and Engineering, ETH Zürich, Mattenstrasse 26, 4058 Basel, Switzerland
[e] European Research Institute for the Biology of Ageing, University of Groningen, University Medical Center Groningen, A. Deusinglaan 1, NL-9713 AV Groningen, The Netherlands

ARTICLE INFO

Keywords:
Differentiation
in situ hybridization
Stylet
Male copulatory apparatus

ABSTRACT

Temporal and spatial characterization of gene expression is a prerequisite for the understanding of cell-, tissue-, and organ-differentiation. In a multifaceted approach to investigate gene expression in the tail plate of the free-living marine flatworm *Macrostomum lignano,* we performed a posterior-region-specific *in situ* hybridization screen, RNA sequencing (RNA-seq) of regenerating animals, and functional analyses of selected tail-specific genes. The *in situ* screen revealed transcripts expressed in the antrum, cement glands, adhesive organs, prostate glands, rhabdite glands, and other tissues. Next we used RNA-seq to characterize temporal expression in the regenerating tail plate revealing a time restricted onset of both adhesive organs and copulatory apparatus regeneration. In addition, we identified three novel previously unannotated genes solely expressed in the regenerating stylet. RNA interference showed that these genes are required for the formation of not only the stylet but the whole male copulatory apparatus. RNAi treated animals lacked the stylet, vesicula granulorum, seminal vesicle, false seminal vesicle, and prostate glands, while the other tissues of the tail plate, such as adhesive organs regenerated normally. In summary, our findings provide a large resource of expression data during homeostasis and regeneration of the morphologically complex tail regeneration and pave the way for a better understanding of organogenesis in *M. lignano*.

1. Introduction

Regeneration and organ formation rely on restricted spatial and temporal gene expression. In recent years, several studies were aimed at the characterization of post-embryonic organogenesis in Platyhelminthes. Members of this phylum are known for their astonishing regeneration abilities, with some species being able to regrow complete animals from small tissue pieces (Morgan, 1901; Reddien and Sanchez Alvarado, 2004). Most regeneration studies were performed in the asexual strains of the freshwater species *Schmidtea mediterranea* and *Dugesia japonica* (reviewed in (Aboobaker, 2011; Adler and Sanchez Alvarado, 2015; Reddien, 2013; Rink, 2013)). Therefore, the molecular program required for the regeneration of most organs of these animals is relatively well-characterized (reviewed in (Roberts-Galbraith and Newmark, 2015)). A common approach to identifying regulatory genes for organ regeneration is to screen annotated transcription factors and genes involved in signaling pathways. In *S. mediterranea*, for example, the epidermal growth factor (EGF) receptor pathway was found to regulate regeneration and homeostasis in the pharynx and eye pigment cells (Fraguas et al., 2011), the gut (Barberan et al., 2016a), and the protonephridia (Barberan et al., 2016b; Rink et al., 2011). Although this approach is often successful, it may lead to a biased selection of candidate genes. Another, unbiased strategy is to characterize the expression profile of defined tissues and to functionally test upregulated transcripts. One elegant way to obtain tissue-specific expression is to purify organs, which has been successfully done with the intestines (Forsthoefel et al., 2012),

* Corresponding author.
E-mail addresses: birgit.lengerer@uibk.ac.at (B. Lengerer), julia.wunderer@uibk.ac.at (J. Wunderer), robert.pjeta@uibk.ac.at (R. Pjeta), giada.carta@i-med.ac.at (G. Carta), damian.kao@gmail.com (D. Kao), aziz.aboobaker@zoo.ox.ac.uk (A. Aboobaker), christian.beisel@bsse.ethz.ch (C. Beisel), e.berezikov@umcg.nl (E. Berezikov), willi.salvenmoser@uibk.ac.at (W. Salvenmoser), peter.ladurner@uibk.ac.at (P. Ladurner).

http://dx.doi.org/10.1016/j.ydbio.2017.07.021
Received 28 April 2017; Received in revised form 21 July 2017; Accepted 27 July 2017
Available online 28 July 2017

cephalic ganglia (Wang et al., 2016), and eyes (Lapan and Reddien, 2012) of *S. mediterranea*. Another practicable method is to amputate the area of interest and to characterize the expression of the regenerating tissue (Adler et al., 2014; Roberts-Galbraith et al., 2016).

In contrast to triclads, few molecular studies have been performed in other taxa of Platyhelminthes. Over recent years, the marine, obligatorily cross-fertilizing hermaphrodite *Macrostomum lignano* has been successfully developed as a model organism (Ladurner et al., 2005b). *M. lignano* belongs to the Macrostomorpha, the most basal group of Rhabditophora (Egger et al., 2015; Laumer et al., 2015). Its small size of around one millimetre and fast generation time of three weeks enables easy culturing within laboratory conditions (Ladurner et al., 2005b). Several methods, including *in situ* hybridization (ISH) (Pfister et al., 2007), RNA interference (Pfister et al., 2008), BrdU (Ladurner et al., 2000), antibody staining (Ladurner et al., 2005a), and transgenesis (Wudarski et al., 2017) have been established. *M. lignano* is able to regenerate its anterior-most region (Egger et al., 2006; Verdoodt et al., 2012) as well as any tissue posterior to the pharynx (Egger et al., 2006). A study focused on the regenerating tail plate demonstrated that the posterior blastema is an accumulation of proliferating neoblasts (Egger et al., 2009). After amputation of the tail plate adhesive organs can be observed in squeeze preparations and stained specimens after just 48 h of regeneration (Egger et al., 2009; Lengerer et al., 2016). Three days after amputation the male copulatory apparatus has begun to rebuild, and the vesicula granulorum and a small stylet are visible. Within the next two to three days the stylet grows to full size and the male copulatory apparatus regains functionality (Egger et al., 2009). Depending on the individual animal, a full set of adhesive organs are regenerated between six to ten days, marking the completion of tail plate regeneration (Egger et al., 2009; Lengerer et al., 2016).

Recently, literature on transcriptome and genome assemblies of *M. lignano* (Grudniewska et al., 2016; Wasik et al., 2015) has been published. A positional RNA sequencing (RNA-seq) analysis was performed by Arbore et al., to identify transcripts specifically expressed in the head-, testis-, ovary-, and tail region. Thereby, a collection of 366 tail-region-specific transcripts were identified (Arbore et al., 2015). Interestingly, a recent study by Ramm et al. has shown that 150 of these transcripts exhibited plasticity of mRNA expression levels depending on their social environment. As part of this study animals were kept alone or in groups of eight. A differential gene expression analysis revealed transcripts up- or downregulated in the larger group size (Ramm et al.). Based on the data of these studies we aimed to identify transcripts involved in regeneration of the tail region.

Here, we present a region-specific *in situ* hybridization screen of 111 transcripts predominately expressed in the posterior region of *Macrostomum lignano*. Using RNA-seq we characterized temporal expression in the regenerating tail plate. The expression of selected transcripts in the regenerating tissues were confirmed with *in situ* hybridization and analysed with RNA interference. Three novel genes were found to be expressed in the regenerating stylet, and their knock-down resulted in animals specifically lacking the male copulatory apparatus.

2. Material and methods

2.1. Animal culture

Macrostomum lignano (Ladurner et al., 2005b) cultures of the inbred line DV1 (Janicke et al., 2013) were kept in petri dishes with nutrient enriched artificial seawater (Guillard's f/2 medium) (Anderson, 2005) and were fed *ad libitum* with the diatom *Nitzschia curvilineata*. Animals were maintained in a climate chamber with 20 °C, 60% humidity and a 14:10 day-night cycle.

2.2. Whole mount in situ hybridization

Whole mount *in situ* hybridization was performed as previously described (Lengerer et al., 2014). Briefly, primers were designed with Primer3 (Untergasser et al., 2012) and a T7 promoter region was added at the 5`end of the reverse primers. Primer sequences are listed in Suppl. Table 1. Template DNA was produced using standard PCR reactions. To synthesize single stranded digoxigenin-labelled RNA probes, T7 polymerase (Promega or Thermo Scientific) and DIG labelling mix (Roche) were used. Anti-digoxigenin-AP Fab fragments (Roche) were diluted 1:2000 and the signal was developed using the NBT/BCIP system (Roche) at 37 °C. Specimen were mounted in Mowiol® 4–88 (Roth, Germany), prepared according to the manufacturer's protocol and images were taken using a Leica DM5000 microscope.

2.3. Sample preparation for RNA-seq

For RNA-seq, tissue samples were collected from 60 worms per sample. The “A” sample included whole regenerating animals (including the regenerating tail). In the “B” sample the regenerating tail was amputated and only the anterior part of the animals was collected for RNA isolation. For the first amputation, 120 adult worms were cut behind developing eggs at the level of cement glands, using a razor blade under a binocular microscope. Afterwards, the worms were transferred to petri dishes containing culture medium and algea. To avoid algea contamination in the RNA samples, animals were starved 16 h prior to the second amputation and fixation. In case of 12 h of regeneration, the amputated animals were not fed after the first amputation. After the given times of regeneration, 60 of the 120 worms were transferred to TRI reagent® (“A”) and 60 were amputated a second time to remove the regenerating tail. The anterior fragments of the twice amputated worms (“B”) were immediately transferred to TRI reagent® (Sigma) and the regenerating tails were discarded. The tissue samples was stored at −80 °C until total RNA extraction, done by TRI reagent/Chloroform extraction. All regeneration experiments were repeated in three replicates.

2.4. Differential gene expression

For the identification of differentially expressed transcripts, six TruSeq Stranded mRNA libraries (Illumina) for every regeneration time point (three biological replicates each of RNA-seq “A” and “B”) were generated. The libraries were sequenced with 50 bp Illumina single reads. However, the quality of the reads of one biological replicate from the timepoints 12 h until day four could not be used for the analysis. The reads of the regeneration time course were mapped to the reference transcriptome (version MLRNA131024, http://www.macgenome.org/download/MLRNA131024/) with Bowtie2 (Langmead and Salzberg, 2012). The data have been deposited with links to BioProject accession number PRJNA381865 in the NCBI BioProject database (https://www.ncbi.nlm.nih.gov/bioproject/). Differentially expressed transcripts were identified using DESeq. 2 (Love et al., 2014). We defined transcripts as differentially expressed between RNA-seq “A” and “B”, if they show a 2-fold difference in the number of mapped reads and a cut off p-value of < 0.01. The list of the transcripts and the corresponding fold change throughout regeneration time course are provided in (Suppl. Table 2).

2.5. RNA interference

RNAi was performed as previously described (Kuales et al., 2011). Briefly, a double-stranded RNA (dsRNA) probe was generated by an *in vitro* transcription system using primer pairs with Sp6 and T7 promoter regions (T7 and SP6 Ribomax™ large scale RNA kit, Promega). DsRNA was diluted in artificial sea water (ASW) to a final

concentration of 15 ng/µl (400 µl per well). The solution was supplemented with algae and with antibiotics (antibiotic concentration: 50 µg/ml). Streptomycin, Kanamycin, and Ampicillin were alternated every day to prevent the selection of resistant bacterial strains. Adult animals were amputated at the level of cement glands and treated with dsRNA during the entire regeneration process. 25 animals were kept in each well of a 12-well plate. Every 24 h, animals were transferred to a clean well plate and the dsRNA solution was changed. Throughout the whole experiment, animals were fed *ad libitum* and were maintained at normal culture conditions (in a climate chamber with 20 °C, 60% humidity and a 14:10 day-night cycle). Here we use *luciferase* dsRNA (Suppl. Fig. 10), or the omission of dsRNA (Fig. 3, Fig. 4, Fig. 5, Suppl. Fig. 8) as controls. As also shown in earlier studies, RNAi treatment had no mock effect on tissue and organ morphology on light- and electron microscopic level (Kuales et al., 2011; Pfister et al., 2008; Sekii et al., 2009). The efficacy of the knockdown was verified by performing whole mount *in situ* hybridization. Phenotypes were documented *in vivo*, after carefully squeezing the animals between a microscope slide and a cover slip. Images were taken using a Leica DM5000 microscope. Selected phenotypes were additionally documented with phalloidin, lectin, and antibody labelling (see next sections).

2.6. Phalloidin and lectin PNA labelling

Animals were relaxed with 7.14% $MgCl_2$ hexahydrate and then fixed in 4% formaldehyde (made from paraformaldehyde) in PBS (PFA) for 1 h. Afterwards the specimen were washed six times 10 min in Tris-buffered saline (pH 8.0) supplemented with 5 mM $CaCl_2$ and 0.1% Triton (TBS-T). Unspecific background staining was blocked by pre-incubation in TBS-T containing 3% *(w/v)* bovine serum albumin (BSA-T) for 1 h at RT. Biotinylated PNA lectin (Vector Laboratories) was diluted 1:200 and applied to the specimen for 2 h at RT. After six washes of 10 min each in TBS-T, the specimen were incubated for 1 h in Dylight488-conjugated-streptavidin (Vector Laboratories) and Phalloidin-Rhodamine both diluted 1:300 in BSA-T at RT (in darkness). After several washing steps in TBS-T, the specimen were mounted in Vectashield and analysed using a Leica DM5000 or Leica SP5 II confocal scanning microscope.

2.7. Macif1 antibody staining

Animals were relaxed with 7.14% $MgCl_2$ hexahydrate and then fixed in 4% formaldehyde (made from paraformaldehyde) in PBS (PFA) for 1 h. Afterwards the specimen were washed several times in PBS and 0.1% Triton (PBS-T) and heated overnight in a 1:10 diluted epitope retrieval solution (DakoCytomation K5336) at 80 °C. After several washing steps with PBS-T, the specimen were blocked in PBS-T containing 1% *(w/v)* bovine serum albumin (BSA-T) for 4 h at 4 °C. Then they were incubated with 1:1000 diluted polyclonal Rabbit-α-macif1 antibody (Lengerer et al., 2016) in 1% BSA-T overnight at 4 °C. After several washes with PBS-T, the specimen were incubated for 1 h in a swine- α-rabbit-FITC antibody diluted 1:500 in BSA-T at room temperature. After several washing steps in PBS-T, the specimen were mounted in Vectashield and analysed using a Leica DM5000 or Leica SP5 II confocal scanning microscope.

2.8. EdU labelling

Intact adults were soaked in the thymidine analogue 5-ethynyl-2′-deoxyuridine (EdU; Invitrogen) at a concentration of 100 µM in artificial seawater for seven days continuously. Afterwards, the animals were relaxed with 7.14% $MgCl_2$ hexahydrate and fixed in 4% PFA for 30 min. The specimen were washed several times with PBS-Triton and blocked with 3% BSA in PBS-T. After several washes in PBS-T, the specimen were incubated in Click-iT® EdU reaction cocktail (concentrations according to manufacturer's instructions – Invitrogen). DNA was visualized with an addition of DAPI (1 µg/ml in PBS-T) for 30 min at room temperature. After several washes with PBS-T, the specimen were mounted in Vectashield (Vector) and analysed using a Leica SP5 II confocal scanning microscope.

3. Results

3.1. Posterior-region-specific in situ hybridization screen

To identify organ-specific expression in the posterior region of *Macrostomum lignano* we performed a medium-scale ISH screen based on the positional transcriptome of Arbore et al. (2015). Briefly, Arbore et al. performed a positional RNA-seq analysis and defined four regions along the anterior-posterior body axis of *M. lignano*: the head-, testis-, ovary-, and tail-region. To obtain region-specific samples, animals were cut at different body regions, and the anterior part was used for RNA-seq. Expression differences between samples were calculated to determine region-specific transcripts (Arbore et al., 2015). For example, transcripts with an at least 4-fold higher expression in the whole animal compared to the region anterior of the developing eggs were considered as potentially tail-region-specific. The so defined tail region contains all tissues posterior to the ovaries, including developing eggs, the female and male genitalia, and adhesive organs (Fig. 1A). To avoid confusion between the terms “tail region” and “tail plate”, we termed this body area “posterior region” within this study. Candidates for the posterior-region-specific ISH were chosen independently of any sequence annotations. The transcripts were selected according to following criteria: (1) transcripts with ≥ 4-fold higher mapped reads in whole animals compared to the region anterior of the developing eggs (putative posterior-region-specific); (2) transcripts with ≥ 50 mapped reads either absolute, or calculated RPK = reads per kilobase in whole animals (to exclude very low expressed transcripts); (3) a length of at least 200 bp, to enable labelling with ISH probes. Overall, 316 transcripts fulfilled these criteria. 150 transcripts changed their expression level due to changes in the social environment, 140 of which were upregulated in larger groups (Ramm et al.). These transcripts were predicted to represent seminal fluid candidates and will be reported elsewhere as part of a project on seminal fluid diversity and function in *M. lignano* (Weber et al.). Finally, 166 transcripts were selected for the present study.

Of the 166 screened transcripts (transcriptome version MLRNA110815), 111 had an expression pattern in whole mount ISH of adult animals (Suppl. Table 1). We classified the spatial expression pattern into seven categories: antrum, cement glands, male copulatory apparatus, adhesive organs, cells enriched in posterior region, posterior region and other tissues, and other pattern (Fig. 1B). Of the transcripts, 34 were expressed in female tissues, including 19 antrum-specific (Fig. 1C, Suppl. Fig. 1) and 15 cement gland-specific (Fig. 1D, Suppl. Fig. 2A-O). The 13 transcripts expressed in the male copulatory apparatus included 11 prostate gland cell-specific (Fig. 1E, Suppl. Fig. 2P-Z) and two with expression in the stylet and the false seminal vesicle (Suppl. Fig. 2AA-AB). 20 transcripts were expressed in the cells of the adhesive organs (Fig. 1F). By the localization of their expression, they were categorized into secretory gland cell-specific (16) (Fig. 1F, Suppl. Fig. 3A-P), anchor cell-specific (3) (Suppl. Fig. 3Q-S), or expression in both secretory gland cells and anchor cells (1) (Suppl. Fig. 3T). The category “cells enriched in posterior region” was used to summarize four different expression patterns. Two transcripts of this category were localized in rhabdite glands, which are distributed over the whole animal but are more numerous in the tail plate (Fig. 1G, Suppl. Fig. 3U,V). One transcript labelled paired cells on the ventral side of the posterior region (Suppl. Fig. 3W). Two transcripts were expressed in a subset of epidermal cells surrounding the whole tail plate (Suppl. Fig. 3X-Y). Beside the expression of the transcripts, these epidermal cells were not distinguishable from other epidermal cells. One staining revealed single cells in the dorsal part of the tail plate (Suppl. Fig. 3Z). The corresponding cell type is currently unknown. The term “posterior region and other

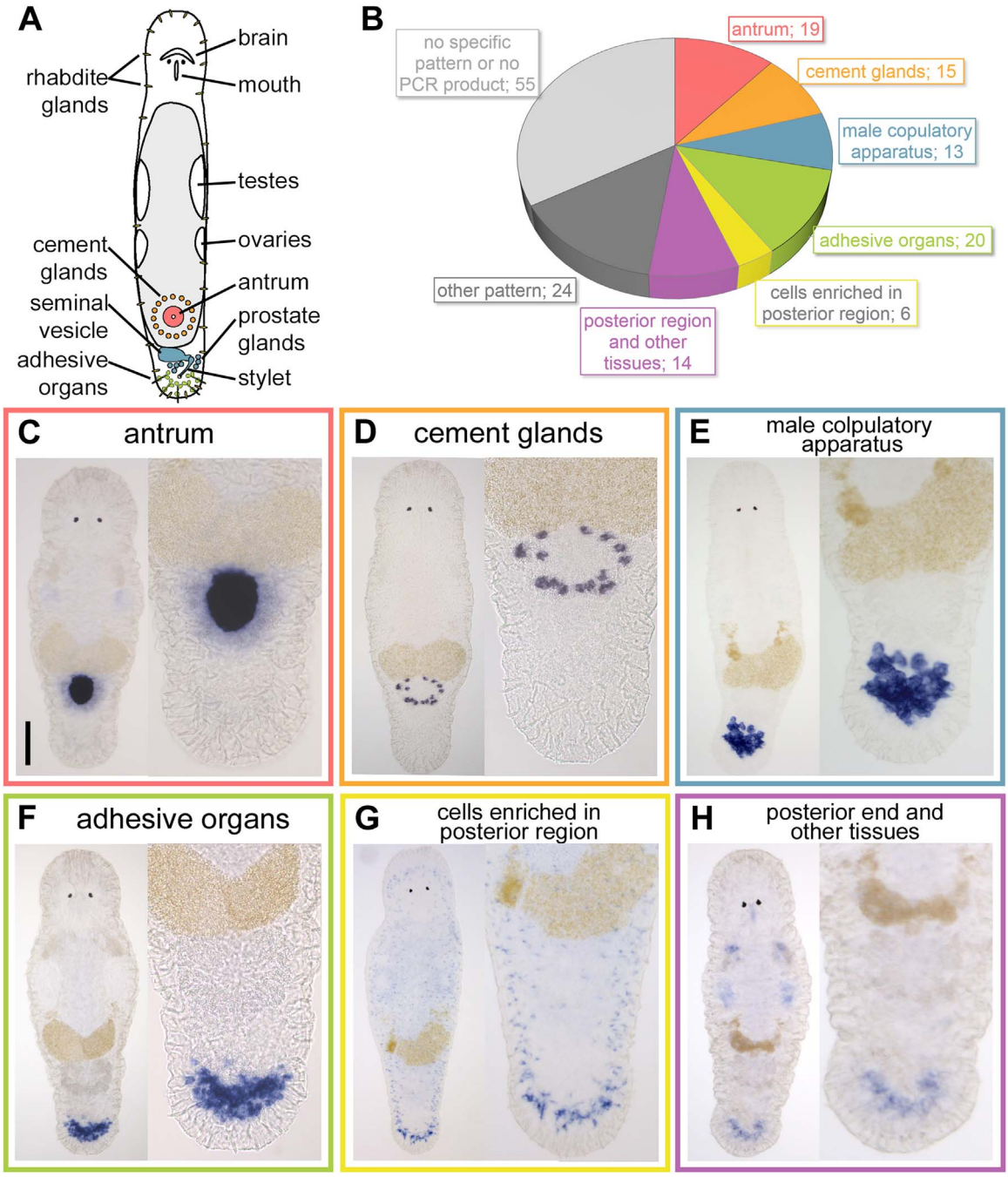

Fig. 1. Overview expression pattern of the posterior region specific *in situ* hybridization screen. (A) Schematic drawing of an adult *Macrostomum lignano*. (B) Pie cart indicating the expression categories and number of transcripts with corresponding *in situ* pattern. (C-H) Exemplary *in situ* hybridizations of the posterior region specific expression categories. Scale bar: 100 µm.

tissues" was used to describe transcripts with an expression in tissues specific for the posterior region and an additional expression in anterior body parts, mostly in the gonads (14) (Fig. 1H, Suppl. Fig. 4). Another 24 transcripts showed non-posterior-region-specific expression pattern (Suppl. Fig. 5), with the majority being expressed in testes, ovaries, or both gonads. For 55 transcripts either no specific primers could be designed (2), the PCR failed (15), or the ISH did not result in a specific staining (38).

3.2. Expression analysis during tail plate regeneration

Next, we aimed to define the expression profile during tail plate regeneration using RNA-seq. In contrast to the positional transcriptome (Arbore et al., 2015), we amputated the animals posterior of the developing eggs at the level of the cement glands. This cutting level was chosen to exclude developing eggs from the amputated tissue and thereby reduce the complexity of expressed mRNA. Furthermore, the same amputation level was used in previous studies on tail plate- (De Mulder et al., 2009; Egger et al., 2009; Nimeth et al., 2007) and adhesive organ- regeneration (Lengerer et al., 2016), which facilitated the comparability of the results. We observed that tail amputation resulted in morphological changes in the anterior part of the animal, especially in the testes and ovaries. Tail-amputated animals stopped sperm production, reduced testes size (personal observation), and altered overall gene expression in the regenerating animal (Wasik et al., 2015). A comparison of regenerating animals with intact ones would represent all expressional changes throughout the whole animal. However, we were interested in the genes exclusively expressed in

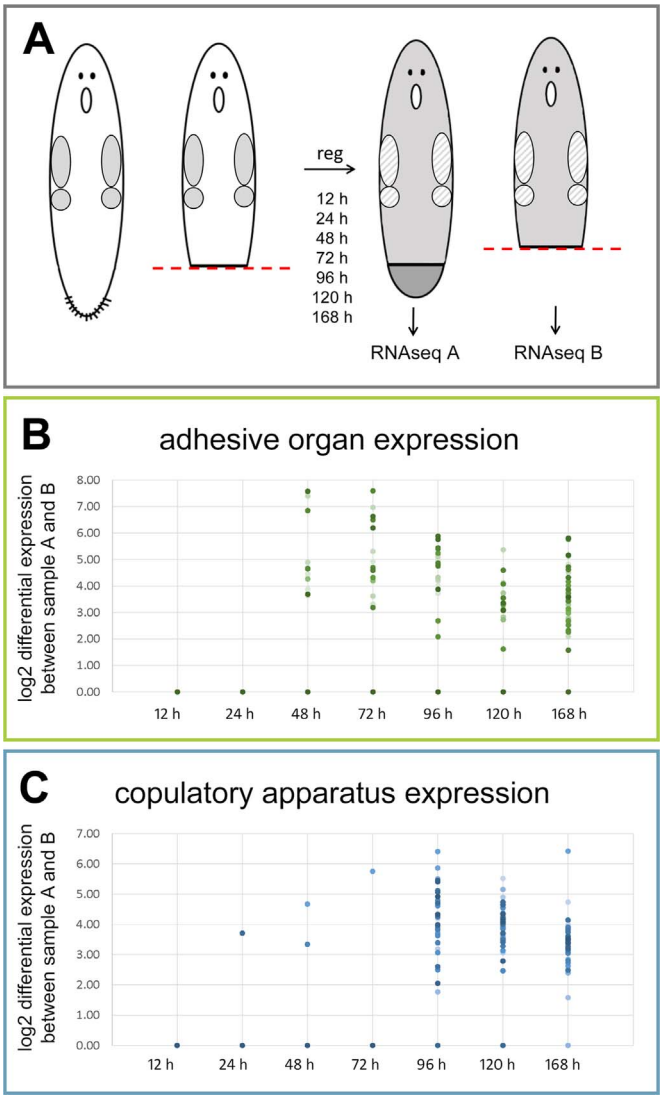

Fig. 2. Amputation scheme used for RNA-seq experiments and exemplary expression of adhesive organ and copulatory apparatus specific transcripts over regeneration time course. (A) Schematic drawing of the amputation scheme used for RNA-seq experiments. (B) Adhesive organs specific transcripts and (C) copulatory apparatus specific transcripts with a differential expression between sample A and B (log2 scale).

the regenerating tail. Due to the small size of the amputated tail fragments, it was not possible to collect these fragments directly, as they tended to disintegrate after amputation. To overcome these limitations, two samples were taken at every regeneration time point (Fig. 2A). Sample A included whole regenerating animals of the respective time point, including the regenerating tail. In sample B, the regenerating tail was amputated, and only the anterior part of the animals was collected for RNA isolation. This experimental setup allowed focus on the expression dynamics, especially within the regenerating area. We defined seven regeneration time points – 12, 24, 48, 72, 96, 120, and 168 h post-amputation - to cover the time required for the formation of all organs specific for the tail plate.

For differential gene expression, RNA was isolated in triplicates of samples A and B for every time point. Illumina libraries were generated, and 50 bp sequencing was performed (see Material and Methods; raw reads available under BioProject accession number PRJNA381865). The generated Illumina reads were mapped to the reference transcriptome available at that time (version MLRNA131024). Because of our interest in organ regeneration, we selected 220 transcripts that exhibited a differential expression (≥ 2-fold, p-value 0.01) in at least two time points between 48 and 168 h of regeneration (Suppl. Table 2, Sheet1). From these, the spatial expression was already known for 186 transcripts based on the posterior-region-specific and seminal fluid ISH screen (Weber et al.). Additionally, 34 novel, differentially expressed transcripts were found in the RNA-seq data (Suppl. Table 2, Sheet1). Notably, 164 transcripts showed expression in the posterior-region-specific and seminal fluid ISH screen (Weber et al.), but they did not show differential expression in the RNA-seq data (Suppl. Table 2, Sheet2). We assume that this resulted from the presence of multiple isoforms in the transcriptome (see discussion).

In previous studies it was shown that after tail plate amputation, adhesive organs start to differentiate after 48 h (Egger et al., 2009; Lengerer et al., 2016). The RNA-seq data corroborated this time course of differentiation and adhesive organ-specific transcripts (MLRNA131024 transcriptome) had increased expression in the tail from 48 h onwards (Fig. 2B). The male copulatory apparatus starts to regenerate at 72 h. At this point, the tip of the stylet is already visible, and in the following two to three days the stylet grows to full size. At the same time, the attached vesicula granulorum, true and false seminal vesicle, and the prostate gland cells are rebuilt (Egger et al., 2009). In our RNA-seq dataset, transcripts of the male copulatory apparatus were upregulated in the tail from 96 h onward (Fig. 2C, Suppl. Fig. 6A). Three transcripts (RNA1310_25676, RNA1310_28866, RNA1310_36278) were also expressed at earlier time points in the RNA-seq dataset. For prostate-specific transcript RNA1310_25676, the temporal and spatial expression during regeneration confirmed the early appearance of the transcript (Suppl. Fig. 6B).

3.3. Spatial and temporal co-expression groups in adhesive organs

The adhesive organs in *M. lignano* consist of three cell types: a supportive anchor cell and two secretory glands - one adhesive and one releasing gland cell (Lengerer et al., 2014; Tyler, 1976). After tail plate amputation, the first adhesive organs differentiate after 48 h (Egger et al., 2009; Lengerer et al., 2016). Over the following days their numbers increase, until they reach their full number of about 130 organs after nine days of regeneration (Egger et al., 2009; Lengerer et al., 2016). Accordingly, all tested secretory gland-specific transcripts (RNA815_13121.1, RNA815_21583, RNA815_23142, RNA815_27695.2, RNA815_48402, RNA1310_81421) and anchor cell-specific transcripts (RNA1310_4919, *macif1*) where expressed in regenerating animals from 48 h onwards after amputation (Fig. 3A-B, Suppl. Fig. 7). Likewise, the expression levels of the transcripts from the *macif1* gene (RNA1310_7834/ RNA1310_9642/ RNA815_3251.1) in the differential RNA-seq data increased after 48 h (Suppl. Table 2, Sheet 1). In addition, we identified one novel anchor cell specific transcript (RNA1310_30724) that encodes for a 144 amino acid long protein containing two EF-hand domains. This transcript showed a characteristic anchor-cell-specific expression profile during regeneration (Fig. 3C).

The transcript RNA1310_47545 showed an unexpected mode of expression with respect to RNA-seq data and ISH patterns. Initially classified as posterior-region-specific in Arbore et al. (Arbore et al., 2015), here we show an expression limited to the ovaries in intact animals (Suppl. Fig. 5M, Fig. 3D1). However, during regeneration the transcript was strongly expressed in the rostrum and in single cells throughout the body (Fig. 3D2-D4). After 48 h of regeneration, an additional expression in the anchor cells was visible (Fig. 3D3-D4).

3.4. Characterization of a new gene required for microvilli formation in anchor cells

To determine their function, all identified anchor cell-specific transcripts (RNA1310_4919, RNA815_51776, RNA815_8153, RNA1310_30724, RNA1310_47545) were analysed with RNA interference (RNAi) during regeneration. As positive control, RNAi of the former described anchor cell-specific *macif1* (Lengerer et al., 2014)

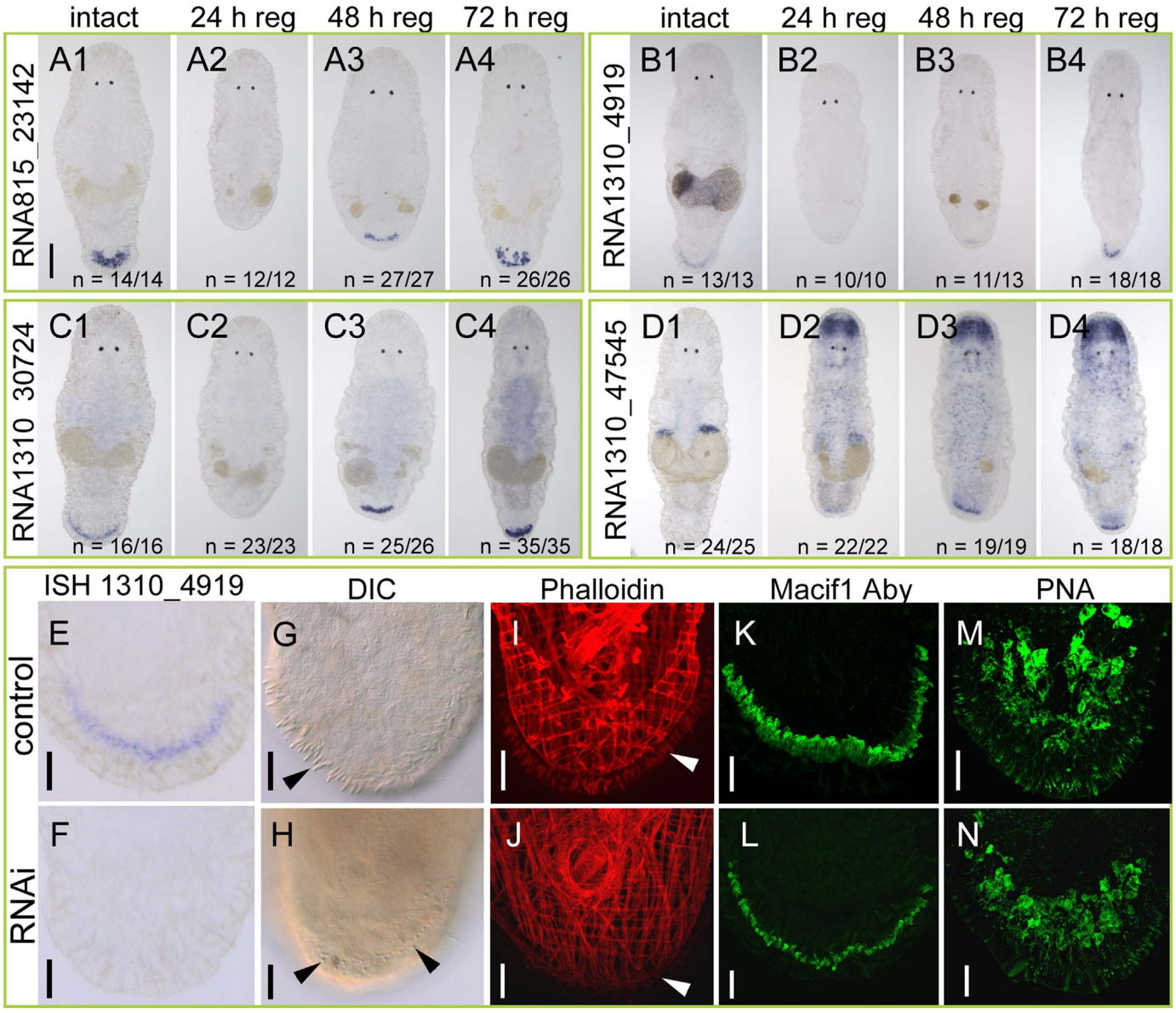

Fig. 3. Expression pattern of adhesive organs specific transcripts in regenerating animals and RNAi phenotype of RNA1310_4919. (A-D) Representative ISH pattern of (A1-4) the secretory gland cell specific transcript RNA815_23142, (B1-4) the anchor cell specific transcripts RNA1310_4919, (C1-4) RNA1310_30724, and (D1-4) RNA1310_47545. (E-N) Tail plate of control- and RNA1310_4919 RNAi treated animals after nine days of regeneration: (E, F) ISH of RNA1310_4919, (G, H) squeeze preparation, (I, J) phalloidin staining, (K, L) Macif1 antibody staining, and (M, N) adhesive gland cell labelling with lectin PNA. Arrowheads highlight the microvilli of anchor cells. Note the shorter microvilli after RNAi treatment. Scale bars: (A) 100 µm, (E-N) 20 µm.

was performed. The ISH after nine days of treatment revealed that all five knock-downs were efficient (data not shown). However, only the knock-down of RNA1310_4919 led to a detectable phenotype (Fig. 3E-N). The RNA1310_4919 RNAi-treated animals showed a non-adhesive phenotype. Squeezing preparations revealed a shortening of their anchor cell specific microvilli (Fig. 3G, H). Furthermore, the microvilli were only weakly stained with phalloidin (Fig. 3I, J), demonstrating a reduction of actin filaments. As these morphological changes strongly resembled the previously described *macif1 (RNAi)* phenotype (Lengerer et al., 2014), we tested if RNA1310_4919 had an effect on the expression of *macif1*. The staining with the available Macif1 antibody (Lengerer et al., 2016) showed no differences between control and RNAi-treated animals (Fig. 3K, L), indicating that RNA1310_4919 does not influence the expression of *macif1*. Also, the labelling of the adhesive vesicles using the lectin PNA (Lengerer et al., 2016) showed no alterations in the adhesive gland cells of RNAi treated animals (Fig. 3M, N).

3.5. Identification of novel genes required for the formation of the male copulatory apparatus

The RNA-seq data revealed six transcripts with a differential expression higher in the tail restricted to 96 and 120 h of regeneration. Two of these transcripts (RNA1310_39915.2 and RNA1310_80800) were socially sensitive expressed and will be reported elsewhere (Weber et al.). For one transcript, no specific primers could be designed (RNA1310_126882). ISH experiments revealed that the expression of the other three transcripts (RNA1310_72446, RNA1310_45118, and RNA1310_51713) was limited to the regenerating stylet (Fig. 4A-C). Stylet formation is completed after post-embryonic development and no expression of the corresponding genes was observed in intact animals (Fig. 4A1, B1, C1). This might be due to a slow homeostatic cell turnover in the stylet. To gain further insight to stylet-related cell renewal in intact adults, we performed seven days continuous EdU exposure. Notably, we have not discovered pronounced accumulation

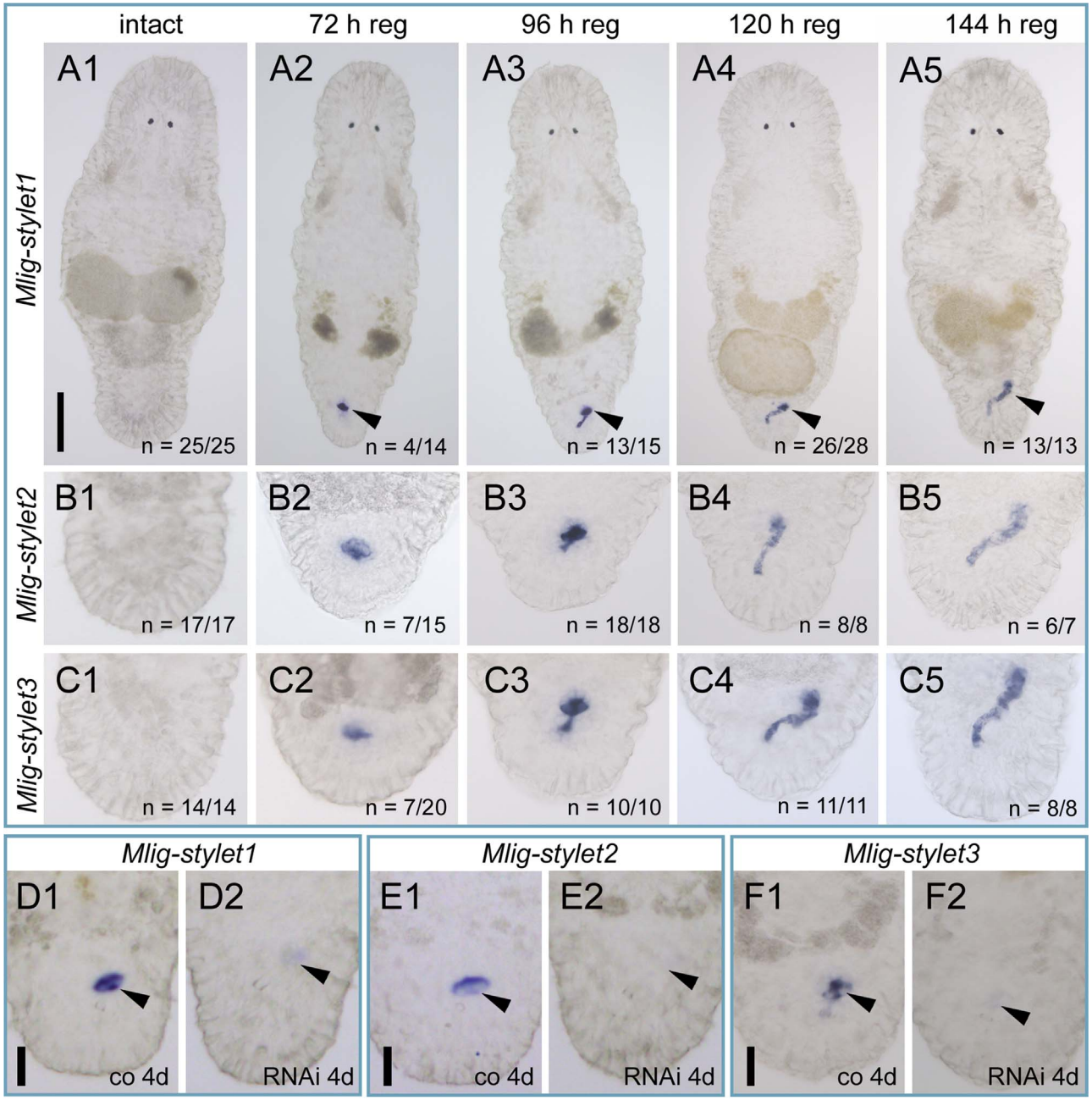

Fig. 4. Whole mount ISH pattern of stylet-specific transcripts in intact, regenerating, and RNAi treated animals. (A-C) Representative ISH pattern of (A1-5) *Mlig-stylet1* (RNA1310_72446), (B1-5) *Mlig-stylet2* (RNA1310_45118), and (C1-5) *Mlig-stylet3* (RNA1310_51713). (D-F) ISH pattern of control and RNAi treated specimen after four days of regeneration of (D1-2) *Mlig-stylet1*, (E1-2) *Mlig-stylet2*, and (F1-2) *Mlig-stylet3*. Arrowheads highlight the regenerating stylet. Scale bars: (A) 100 μm; (D-F) 20 μm.

of EdU-positive cells in the stylet region (in 38 out of 39 animals) (Suppl. Fig. 8A1–4), indicating that the cells of the stylet were not renewed within this time. This is in contrast to a newly forming copulatory apparatus (seen in 1 out of 39 animals) (Suppl. Fig. 8B1–4), which can occur when animals lose their stylet. From these results we conclude that there is very slow cell turnover in the stylet. This observation was also supported by long term RNAi experiments in intact animals (see next sections).

No homologues proteins were found using BLAST search (blastx) (Altschul et al., 1997) against available protein databases for all three sequences (Suppl. Table 3). Based on their expression pattern, we refer to the three transcripts as *Mlig-stylet1* (RNA1310_72446), *Mlig-stylet2* (RNA1310_45118), and *Mlig-stylet3* (RNA1310_51713). To evaluate their function, we soaked tail-amputated animals in dsRNA until the regeneration was completed after nine days. To confirm the knock-down, a subset of 10 animals were fixed after four days of treatment and whole mount ISH was performed. All transcripts were efficiently knocked down after four days of regeneration (Fig. 4D1-F2). The single knock-down of *Mlig-stylet1* and *Mlig-stylet3* led to knock-down phenotypes in the male copulatory apparatus of varying shape and frequency (Table 1). The strongest phenotype resulted in individuals missing all parts of the male copulatory apparatus (Fig. 5A). This severe morphological phenotype was observed in squeezing preparations of living animals (Fig. 5B, E). In contrast to control animals (Fig. 5B), treated animals had no stylet, vesicula granulorum, true and false seminal vesicle, or prostate gland cells (Fig. 5E). Phalloidin staining confirmed the absence of the muscular seminal vesicle, vesicula granulorum, and the muscles associated with the stylet (Fig. 5C, F). According to the loss of prostate gland cells, the expression of prostate genes was also diminished (Fig. 5D, G). Moreover, the

Table 1
Summary of shape and frequency of phenotypes, observed after nine days of RNAi against *Mlig-stylet* transcripts during tail plate regeneration.

	Normal	No copulatory apparatus	Only vesicula granulorum and tip of stylet	Stylet of half size
Control	**100%** (50/50)	**0%**	**0%**	**0%**
Milg-stylet1 (RNAi)	**44.7%** (21/47)	**12.8%** (6/47)	**21.3%** (10/47)	**21. 3%** (10/47)
Milg-stylet2 (RNAi)	**95.2%** (40/42)	**2.4%** (1/42)	**0%**	**2.4%** (1/42)
Milg-stylet3 (RNAi)	**55.8%** (24/43)	**2.3%** (1/43)	**20.9%** (9/43)	**20.9%** (9/43)
Milg-stylet1 + Milg-stylet2 (RNAi)	**17.3%** (9/52)	**25.0%** (13/52)	**21.2%** (11/52)	**36.5%** (19/52)
Milg-stylet1 + Milg-stylet3 (RNAi)	**16.7%** (8/48)	**41.7%** (20/48)	**16.7%** (8/48)	**25.0%** (12/48)
Milg-stylet2 + Milg-stylet3 (RNAi)	**55.0%** (22/40)	**15.0%** (6/40)	**5.0%** (2/40)	**25.0%** (10/40)

absence of the male copulatory apparatus in the tail plate also affected the sperm production and testis size. In control animals, the testis was full with developing and mature sperm (Fig. 5H). In contrast, no sperm production could be observed in individuals missing the male copulatory apparatus, resulting in smaller testis size (Fig. 5I). In 15 out of 22 investigated individuals missing a copulatory apparatus, received sperm in the female antrum were present (Suppl. Fig. 8C). Furthermore, in 21 of 22 animals developing eggs were present. These results indicate that the animals can copulate and receive sperm in absence of an own male copulatory apparatus. *Mlig-stylet1 (RNAi)* and *Mlig-stylet3 (RNAi)* also resulted in less pronounced phenotypes (Table 1), like individuals with a visible vesicula granulorum and the tip of the stylet (Suppl. Fig. 8D) or a stylet with only about half of the normal length (Suppl. Fig. 8E). In these animals, the morphology of the copulatory apparatus resembled control animals after three or four days of regeneration in an otherwise completely regenerated tail plate (Suppl. Fig. 8D, E). Around half of the animals in both treatment groups regenerated in a normal way (Table 1).

Simultaneous RNAi treatment against two stylet-specific transcripts resulted in an increased frequency of the phenotypes (Table 1). The co-treatment with *Mlig-stylet2* dsRNA increased the number of treatment phenotypes for both of the other stylet transcripts, although single treatment against *Mlig-stylet2* had no visible effect (Table 1). The highest frequency of animals lacking the male copulatory apparatus

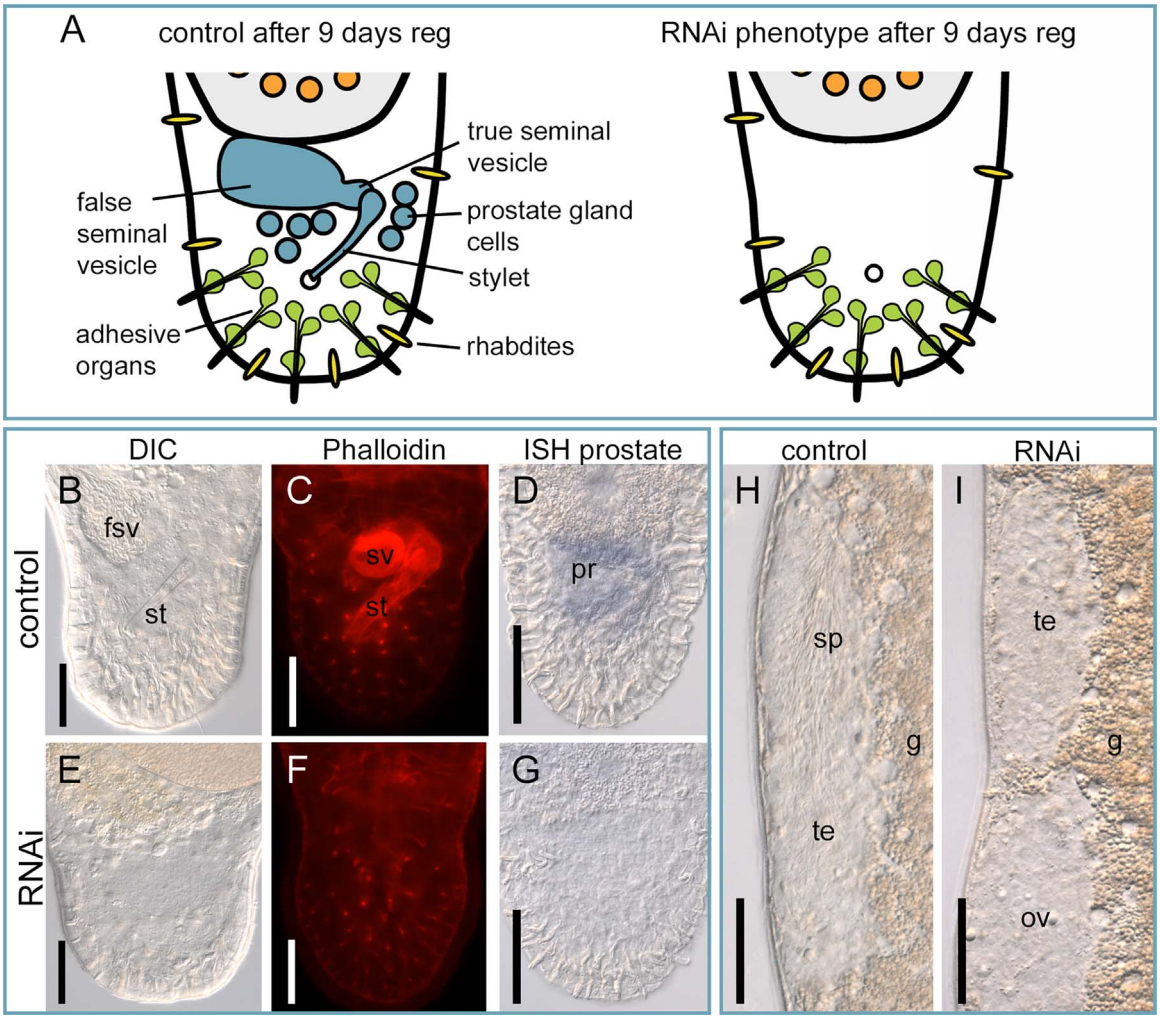

Fig. 5. RNAi phenotype of stylet-specific transcripts. (A) Schematic drawings of the tail plate of control and RNAi treated animals. (B-G) Tail plate of control- and RNAi treated animals *(Mlig_stylet1 + Mlig_stylet2)* after nine days regeneration: (B, E) squeeze preparation, (C, F) phalloidin staining, and (D, G) ISH pattern of prostate transcript RNA815_15018.1. Note that all parts of the male copulatory apparatus are missing in the RNAi animals. (H) Testis of a control animal. (I) Testis and ovary of an RNAi animal *(Mlig_stylet1 + Mlig_stylet2)*. Note the small size of the testis and the absence of sperm. *fsv* false seminal vesicle, *g* gut, *ov* ovaries, *pr* prostate, *sp* sperm, *st* stylet, *sv* seminal vesicle, *te* testes. Scale bars: (B-I) 50 μm.

(41.7%) after nine days was achieved by the combined treatment of *Mlig-stylet1* and *Mlig-stylet3* dsRNA (Table 1). Next, we explored if the lack of the male copulatory apparatus is due to the absence of an organ primordium or if a primordium is formed and breaks down later. Therefore, we performed simultaneous RNAi treatment of *Mlig-stylet1* and *Mlig-stylet3* and quantified the presence of a visible male copulatory primordia after three or four days in live squeeze preparations (Suppl. Fig. 8F). In 64 out of 65 animals a primordium was present. However, after nine days 13 out of 55 animals (10 animals were lost during manipulation) completely lacked the male copulatory apparatus. From this finding we conclude that the expression of the *Mlig-stylet* genes is not required for primordium formation, but for the differentiation of the male copulatory apparatus. Further, we were asking whether the expression of the *Mlig-stylet* genes influenced each other. For that reason, we performed RNAi and ISH of all three *Mlig-stylet* genes and found that their expression is independent (Suppl. Fig. 9). Next, we evaluated if animals lacking the copulatory apparatus can recover from the RNAi treatment. Therefore, we transferred animals lacking the copulatory apparatus after nine days of regeneration and RNAi treatment *(Mlig-stylet1 + Mlig-stylet2)* to normal culture medium. Five days after the end of the treatment, all animals had regenerated a stylet, and the testes produced sperm (5 out of 5). This indicated that immediately after the end of the dsRNA treatment, the missing structures started to regenerate. Therefore, the copulatory apparatus can be regenerated in the otherwise fully developed tail plate. To evaluate if RNAi also affected an existing stylet in an intact adult worm, we treated adults for 22 days with *Mlig-stylet1* and *Mlig-stylet3* dsRNA. All animals (44 out of 44) showed a normal stylet phenotype at the end of the treatment period.

4. Discussion

4.1. Selection of transcripts for the posterior-region-specific ISH screen

The knowledge of spatial and temporal expression pattern is essential to understanding the molecular mechanism controlling tissue maintenance and regeneration. Therefore, large-scale ISH screens have been performed in most model organisms, such as mouse (Eichele and Diez-Roux, 2011; Lein et al., 2007; Neidhardt et al., 2000), chicken (Bell et al., 2004; Darnell et al., 2007), zebrafish (Kudoh et al., 2001; Thisse and Thisse, 2008), *Xenopus* (Pollet et al., 2005; Pollet and Niehrs, 2001), *Drosophila* (Frise et al., 2010; Molnar et al., 2012; Tomancak et al., 2002; Weiszmann et al., 2009), and *Ciona intestinalis* (Imai et al., 2006; Miwata et al., 2006). In Platyhelminthes, large expressional datasets are available for *Schmidtea mediterranea* (Forsthoefel et al., 2012; Lapan and Reddien, 2012; Roberts-Galbraith et al., 2016; Sanchez Alvarado et al., 2002; Thi-Kim Vu et al., 2015). In most members of this phylum, expression analysis is either missing or limited to a low number of genes, such as in *Schistosoma mansoni* (Rofatto et al., 2012; Wang and Collins, 2016; Wilson et al., 2015), *Dugesia japonica* (Hwang et al., 2015; Pang et al., 2016; Shibata et al., 2012), or *Macrostomum lignano* (Grudniewska et al., 2016; Kuales et al., 2011; Pfister et al., 2007). The study on positional RNA-seq in *M. lignano* by Arbore et al. provided a resource for further analysis of spatially restricted cell-, tissue-, and organ-specific-genes (Arbore et al., 2015). However, only exemplary transcripts were shown for the different regions. Out of the 366 posterior-region-specific transcripts, three were confirmed to show a tail-specific expression (Arbore et al., 2015). Yet the posterior region of *M. lignano* holds a variety of tissues and organs involved in reproduction and adhesion. Regarding our interest in reproductive organs and adhesion of *M. lignano*, we aimed to screen the expression of all posterior-region-specific transcripts by ISH. In order to distribute the screening workload between our lab and the Ramm lab (University of Bielefeld), a further selection of transcripts was made. The Ramm lab is focused on seminal fluid-related transcripts, while our lab is interested in developmental genes and genes involved in egg and animal adhesion. In a recent study, Ramm et al. showed that 150 posterior-region-specific transcripts exhibited increased expression levels with respect to group size (Ramm et al.). The majority of these transcripts are upregulated in groups of eight animals, compared to solitary animals. As prostate gland cells are present in the posterior region, it was predicted that these social-sensitive transcripts are involved in seminal fluid production (Ramm et al.). Therefore, all 150 differentially expressed transcripts in the posterior region were screened in a study targeted at the identification of seminal fluid proteins by the Ramm lab (Weber et al.). Many indeed showed expression in the prostate glands (Weber et al.), proving the adequacy of the seminal-fluid protein selection. For the ISH screen we selected posterior-region-specific transcripts that did not show plastic expression according to the social environment (see first section of results), which encompass expression in the reproductive organs, cement glands, adhesive organs, and rhabdite glands.

4.2. Methodological considerations: transcriptomes, strategy of amputation, RNA-seq analysis

The positional RNA-seq approach by Arbore et al. (Arbore et al., 2015) was based on the transcriptome "MLRNA110815" available at that time and containing 76,437 contigs. Likewise, the ISH screen presented here is based on this transcriptome version. The RNA-seq regeneration time course dataset was generated when a new version of a *M. lignano* transcriptome was available (MLRNA131024; 174,922 contigs). This version had improvements regarding assembly strategy, contig length, CEGMA coverage, and isoform content (Simanov, 2014). Therefore, we decided to map the RNA-seq reads against the new transcriptome. However, one has to take into account that the two transcriptomes do not show a 1:1 transcript correlation. Rather, the increased number of contig isoforms led to the fact that multiple transcripts of the MLRNA131024 transcriptome often correspond to one transcript of the MLRNA110815 transcriptome. Thus, for example, transcript RNA815_31710 from the MLRNA110815 transcriptome relates to transcripts RNA1310_20970, RNA1310_22602, and RNA1310_23356 from the MLRNA131024 transcriptome (Suppl. Table 2). In order to avoid any confusion, both transcript names are included in the figures and tables.

Upon tail plate amputation, the circular and longitudinal muscles contract to close the wound, and the epidermal cells flatten to cover the wound surface. Due to the muscular contractions, the early formed blastema is bent to the ventral side and remains in this position until about 24 h post amputation (Egger et al., 2009). This early blastema is very fragile and tends to disintegrate when it is amputated. Therefore, we did not collect the regenerating tail directly but decided to perform a differential approach, comparing regenerating animals with and without the regenerating tail (Fig. 2). However, this approach might not allow the identification of tail plate expressed genes with additional expression in the anterior part of the animals. In such cases, the increase of expression during regeneration in the tail plate does not compensate for the high expression in the anterior part. For this reason, stem cell-specific genes like piwi and vasa did not show up in the differential RNA-seq. Additionally, the reads were mapped to the unclustered transcriptome version that was available at the time (MLRNA131024), which contains a high number of transcripts (174,922). This high number is due to multiple variants of one transcript. In such cases, mapping of reads results in a dilution in the number of reads across the transcript variants. This can lead to a false-negative differential expression in the RNA-seq data. Recently, an improved transcriptome version ML150904 was published containing less than half that number of transcripts (60,180) (Grudniewska et al., 2016). Even in this improved transcriptome, more than half of the genes were found to be

duplicated (Grudniewska et al., 2016), reflecting chromosome duplication events in the used *M lignano* DV1 line (Zadesenets et al., 2016).

4.3. Tissue and organ specific expression in the posterior-region

In our posterior-region-specific ISH screen, a variety of molecular markers for different tissues, cells, and organs were identified. The posterior region contains the structures of the male and female genitalia, as well as the adhesive organs. Out of the 13 transcripts specific for the male copulatory apparatus, 11 were expressed in prostate gland cells (Suppl. Fig. 2P-Z), and those transcripts were not upregulated in the social RNA-seq screen (Ramm et al.). Our attempt to knock-down one of the non-differentially expressed transcripts (RNA1310_25676), which is one of the earliest expressed prostate-specific transcripts in regenerating animals, did not lead to a reduction of the mRNA level. Therefore, future studies are necessary to evaluate the function of the identified prostate-specific-transcripts.

We identified 19 transcripts specific for the antrum (Suppl. Fig. 1) and 15 transcripts expressed in the cement gland cells (Suppl. Fig. 2A-O). When an egg matures, it migrates into the female antrum. The female opening is surrounded by the cement gland cells. It was proposed that the secretions of cement gland cells form the outer layer of the egg shell and provide the permanent glue that attaches the egg to the substratum (Ladurner et al., 2005b). A similar shell formation was described in polyclad flatworms (Ishida, 1989, 1986). Our list of transcripts expressed in the antrum and cement gland cells now allows characterization of the genes required for egg shell formation and the proteinaceous components of the permanent adhesive. Future investigations based on this data will help to describe the mode of egg shell formation and to identify novel adhesive proteins.

Currently we are investigating the adhesive secretions of the duo-gland adhesive system in a multidisciplinary project aimed at the characterization of temporary marine adhesives. A comprehensive functional analysis of secreted adhesive proteins identified here will be presented elsewhere. In the current study, we therefore concentrated on the function of anchor-cell-specific transcripts. Overall, six transcripts with an expression in the anchor cells during homeostasis and/or regeneration were identified (Suppl. Fig. 3Q-T, Fig. 3B-D). The knock-down of RNA1310_4919 led to severe morphological changes of the anchor cells and resulted in a non-adhesive phenotype (Fig. 3E-N). The sequence of RNA1310_4919 encodes for a 953 amino acid long formin-like protein, with a FH2 domain at its C-terminal end (Interpro) (Finn et al., 2017). Formins are known to regulate actin filament elongation and to catalyse the assembly of long filaments. The FH2 domains dimerize and form a donut-shaped ring that binds to barbed ends of actin filaments. Formin-dimers stay attached to the barbed ends during the elongation and generate long, unbranched bundles of actin filaments (reviewed in (Carlier et al., 2015; Grikscheit and Grosse, 2016; Shekhar et al., 2016)). The expression of the formin-like RNA1310_4919 was restricted to the anchor cells of adhesive organs (Suppl. Fig. 3Q, Fig. 3B,E). RNAi-mediated knock-down led to shortened anchor-cell-specific microvilli with reduced actin filament bundles (Fig. 3G-J). The phenotype depicted the formerly described RNAi phenotype of the intermediate filament *macif1* (Lengerer et al., 2014), but it did not affect the expression of the latter (Fig. 3K-L). Due to the cell-type specific expression and the RNAi phenotype, we assume that the identified formin-like protein RNA1310_4919 is required for the elongation of actin bundles in the anchor-cell-specific microvilli. The phenotype corroborated the relevance of the structural integrity of the anchor-cell-specific microvilli during the adhesion process (Lengerer et al., 2014).

Additionally, the posterior-region-specific ISH screen revealed so far undescribed cell types (Suppl. Fig. 3W-Z). Based on their shape and location, the paired cells in the posterior region could represent nerve cell bodies (Suppl. Fig. 3W) (Ladurner et al., 2005a; Morris et al., 2007). Two transcripts were expressed in a subset of epidermal cells in the tail plate (Suppl. Fig. 3X-Y), which were morphologically undistinguishable from other epidermal cells. Also, the cell types corresponding to the labelled cells in the tail plate and single cells posterolateral to the pharynx could not be identified (Suppl. Fig. 3Z). In summary, the large number of expression patterns pave the way for future studies of the different organs and cells.

4.4. Identification and characterization of stylet-specific genes

Previous studies in freshwater flatworms showed that the expression of genes required for organogenesis is often maintained in fully developed organs (Adler et al., 2014; Forsthoefel et al., 2012; Fraguas et al., 2011; Lapan and Reddien, 2011, 2012; Rink et al., 2011). In our regeneration RNA-seq dataset, the majority of transcripts upregulated in regenerating tails were also expressed in the tail plate of homeostatic animals (Suppl. Fig. 2, Sheet 1). Only a small proportion of transcripts were exclusively expressed during tail regeneration (Suppl. Fig. 2, Sheet 1). Among those, we identified three novel stylet-specific genes with a restricted expression in the forming stylet (Fig. 4A1-C5). The down-regulation of these transcripts led to regeneration defects in the male copulatory apparatus. The most severe phenotype was the complete absence of any tissues of the male copulatory apparatus, including stylet, true and false seminal vesicle, and prostate glands (Fig. 5). RNAi and ISH revealed that the knockdown of one *Mlig-stylet* gene had no visible effect on the expression of the other two *Mlig-stylet* genes (Suppl. Fig. 9). The variation of phenotype shapes and occurrence could be the result of incomplete knock-down and/or other redundant genes that were not identified (Table 1, Fig. 5). Interestingly, animals treated with dsRNA of *Mlig-stylet1* and *Mlig-stylet3* formed a visible male copulatory apparatus primordium after three and four days (Suppl. Fig. 8F). After prolonged RNAi treatment (nine days), animals lacking the male copulatory apparatus showed no signs of a primordium anymore (Fig. 5). This may indicate that the *Mlig-stylet* genes are not initially required for the formation of the primordium, but for the differentiation of the cells of the male copulatory apparatus. When the male copulatory apparatus fails to be formed, the primordium seems to disintegrate. Nevertheless, as no conserved domains or any homology to other proteins was identified, the specific function of the stylet-specific genes remains elusive.

In *Macrostomum lignano* approximately one third of all cells are renewed within two weeks (Nimeth et al., 2002). After seven days continuous EdU treatment of intact animals, no EdU-positive cells in the area of the stylet were present (Suppl. Fig. 8A). Accordingly, the knockdown of *Mlig-stylet1* and *Mlig-stylet 3* for three weeks in intact adults led to no stylet phenotype. Both indicates that once the male copulatory apparatus is formed, the cell turnover in the stylet happens very slowly. Previous findings showed, that in mass culture occasionally adults without a functional stylet can be found (Schärer and Vizoso, 2007). It was observed that adult animals can lose their stylet, which is rebuild after the loss (L. Schärer pers. comm.). In accordance to this observation, we identified one individual that was rebuilding the stylet at the time of the fixation, resulting in an accumulation of EdU-positiv cells at the area (Suppl. Fig. 8B).

Reparative regeneration is thought to be initiated as a response to a traumatic injury (reviewed in (Erler and Monaghan, 2015)). An interesting aspect of the copulatory apparatus is that upon the stop of the RNAi treatment, the missing copulatory apparatus regenerated within the otherwise complete tail plate. LoCascio et al. proposed a model for passive tissue regeneration through constant progenitor production that could explain this phenomena (LoCascio et al., 2017). However, the proposed model requires a constant rate of homeostatic cell turnover, which seems not to be the case in the stylet of *M. lignano*. At the moment it remains unclear how the absence of the stylet triggers its formation in an intact tail plate. It may be that the restoration of the copulatory apparatus does not require a regenerative trigger but recapitulates regular post-embryonic development.

Several studies in *M. lignano* were aimed at the investigation of sex allocation and resulting phenotypic plasticity (Janicke et al., 2013; Schärer, 2009; Schärer and Ladurner, 2003). The RNAi phenotype of animals lacking the male copulatory apparatus provides a new tool to study behaviour and transcriptomic consequences of hermaphrodites artificially depleted of their male function. Additional to the lack of the male copulatory apparatus, the RNAi-treated animals consequently did not restore their sperm production during regeneration. This resulted in smaller testes without any mature sperm. In future studies, this severe morphological phenotype could be used to distinguish mRNAs expressed specifically within the male reproductive system. For example, in *S. mediterranea*, RNAi of *Six1/2-2* and *POU2/3* was used to deplete the protonephridia and to compare the expression between RNAi-treated animals and controls (Scimone et al., 2011), by which the key regulatory genes for protonephridia regeneration and essential proteins for their function in excretion and osmoregulation were identified. A similar approach in *M. lignano* using *Mlig-stylet (RNAi)* would allow the identification of genes responsible for organogenesis of the male copulatory apparatus, sperm production, and prostate seminal fluid proteins.

5. Conclusions

Altogether, our expression analysis of posterior-region-specific transcripts during homeostasis and regeneration provide a valuable resource for future studies on flatworm biology. The described molecular markers for various organs will pave the way for investigations on genes involved in permanent and reversible adhesion, copulation, reproduction, and egg formation. Furthermore, we identified three novel genes required for organogenesis of the male copulatory apparatus. With the advent of transgenesis in *M. lignano*, the expression patterns described here will support the molecular characterization of cell-, tissue-, and organ-specific differentiation. The data provided here enables comparative analysis of regeneration between flatworm species and beyond the Platyhelminthes.

Competing interests

The authors declare that they have no competing interests.

Contributions

BL, JW, RP, and GC performed ISH and RNAi experiments and interpreted data. DK and AA analysed sequencing data and performed the differential gene expression analysis. CB conceived sequencing experiments and contributed sequencing data. EB contributed previously unpublished transcriptome data. WS helped interpreting ISH and RNAi data. PL and BL conceived and designed the study and wrote the paper. All authors read and approved the final manuscript.

Funding

The project is supported by Austrian Science Fund (FWF): [P 25404-B25]. BL was a recipient of a DOC Fellowship of the Austrian Academy of Sciences and is supported by a PhD Fellowship of the University of Innsbruck (24020). RP was supported by a PhD Fellowship of the University of Innsbruck. DK and AAA were funded by BBSRC grant BB/K007564/1.

Acknowledgements

We thank L. Schärer for his help in designing the RNA-Seq sampling strategy, which was motivated by his desire to learn about genes involved in copulatory stylet formation. We thank the anonymous reviewers for their comments and suggestions that helped to improve the manuscript.

Appendix A. Supporting information

Supplementary data associated with this article can be found in the online version at doi:10.1016/j.ydbio.2017.07.021.

References

Aboobaker, A.A., 2011. Planarian stem cells: a simple paradigm for regeneration. Trends Cell Biol. 21, 304–311.
Adler, C.E., Sanchez Alvarado, A., 2015. Types or states? Cellular dynamics and regenerative potential. Trends Cell Biol. 25, 687–696.
Adler, C.E., Seidel, C.W., McKinney, S.A., Sanchez Alvarado, A., 2014. Selective amputation of the pharynx identifies a FoxA-dependent regeneration program in planaria. Elife 3, e02238.
Altschul, S.F., Madden, T.L., Schaffer, A.A., Zhang, J., Zhang, Z., Miller, W., Lipman, D.J., 1997. Gapped BLAST and PSI-BLAST: a new generation of protein database search programs. Nucleic Acids Res. 25, 3389–3402.
Anderson, R.A., 2005. Algal Culturing Techniques. Elsevier Academic Press, Burlington, San Diego, London.
Arbore, R., Sekii, K., Beisel, C., Ladurner, P., Berezikov, E., Schärer, L., 2015. Positional RNA-Seq identifies candidate genes for phenotypic engineering of sexual traits. Front. Zool. 12, 14.
Barberan, S., Fraguas, S., Cebria, F., 2016a. The EGFR signaling pathway controls gut progenitor differentiation during planarian regeneration and homeostasis. Development 143, 2089–2102.
Barberan, S., Martin-Duran, J.M., Cebria, F., 2016b. Evolution of the EGFR pathway in Metazoa and its diversification in the planarian *Schmidtea mediterranea*. Sci. Rep. 6, 28071.
Bell, G.W., Yatskievych, T.A., Antin, P.B., 2004. GEISHA, a whole-mount in situ hybridization gene expression screen in chicken embryos. Dev. Dyn.: Off. Publ. Am. Assoc. Anat. 229, 677–687.
Carlier, M.F., Pernier, J., Montaville, P., Shekhar, S., Kuhn, S., Cytoskeleton, D., Motility, g., 2015. Control of polarized assembly of actin filaments in cell motility. Cell Mol. Life Sci. 72, 3051–3067.
Darnell, D.K., Kaur, S., Stanislaw, S., Davey, S., Konieczka, J.H., Yatskievych, T.A., Antin, P.B., 2007. GEISHA: an in situ hybridization gene expression resource for the chicken embryo. Cytogenet. Genome Res. 117, 30–35.
De Mulder, K., Pfister, D., Kuales, G., Egger, B., Salvenmoser, W., Willems, M., Steger, J., Fauster, K., Micura, R., Borgonie, G., Ladurner, P., 2009. Stem cells are differentially regulated during development, regeneration and homeostasis in flatworms. Dev. Biol. 334, 198–212.
Egger, B., Ladurner, P., Nimeth, K., Gschwentner, R., Rieger, R., 2006. The regeneration capacity of the flatworm *Macrostomum lignano* -on repeated regeneration, rejuvenation, and the minimal size needed for regeneration. Dev. Genes Evol. 216, 565–577.
Egger, B., Gschwentner, R., Hess, M.W., Nimeth, K.T., Adamski, Z., Willems, M., Rieger, R., Salvenmoser, W., 2009. The caudal regeneration blastema is an accumulation of rapidly proliferating stem cells in the flatworm *Macrostomum lignano*. BMC Dev. Biol. 9, 41.
Egger, B., Lapraz, F., Tomiczek, B., Muller, S., Dessimoz, C., Girstmair, J., Skunca, N., Rawlinson, K.A., Cameron, C.B., Beli, E., Todaro, M.A., Gammoudi, M., Norena, C., Telford, M.J., 2015. A transcriptomic-phylogenomic analysis of the evolutionary relationships of flatworms. Curr. Biol. 25, 1347–1353.
Eichele, G., Diez-Roux, G., 2011. High-throughput analysis of gene expression on tissue sections by in situ hybridization. Methods 53, 417–423.
Erler, P., Monaghan, J.R., 2015. The link between injury-induced stress and regenerative phenomena: a cellular and genetic synopsis. Biochim. Biophys. Acta 1849, 454–461.
Finn, R.D., Attwood, T.K., Babbitt, P.C., Bateman, A., Bork, P., Bridge, A.J., Chang, H.Y., Dosztanyi, Z., El-Gebali, S., Fraser, M., Gough, J., Haft, D., Holliday, G.L., Huang, H., Huang, X., Letunic, I., Lopez, R., Lu, S., Marchler-Bauer, A., Mi, H., Mistry, J., Natale, D.A., Necci, M., Nuka, G., Orengo, C.A., Park, Y., Pesseat, S., Piovesan, D., Potter, S.C., Rawlings, N.D., Redaschi, N., Richardson, L., Rivoire, C., Sangrador-Vegas, A., Sigrist, C., Sillitoe, I., Smithers, B., Squizzato, S., Sutton, G., Thanki, N., Thomas, P.D., Tosatto, S.C., Wu, C.H., Xenarios, I., Yeh, L.S., Young, S.Y., Mitchell, A.L., 2017. InterPro in 2017-beyond protein family and domain annotations. Nucleic Acids Res. 45, D190–D199.
Forsthoefel, D.J., James, N.P., Escobar, D.J., Stary, J.M., Vieira, A.P., Waters, F.A., Newmark, P.A., 2012. An RNAi screen reveals intestinal regulators of branching morphogenesis, differentiation, and stem cell proliferation in planarians. Dev. Cell 23, 691–704.
Fraguas, S., Barberan, S., Cebria, F., 2011. EGFR signaling regulates cell proliferation, differentiation and morphogenesis during planarian regeneration and homeostasis. Dev. Biol. 354, 87–101.
Frise, E., Hammonds, A.S., Celniker, S.E., 2010. Systematic image-driven analysis of the spatial Drosophila embryonic expression landscape. Mol. Syst. Biol. 6, 345.
Grikscheit, K., Grosse, R., 2016. Formins at the junction. Trends Biochem. Sci. 41, 148–159.
Grudniewska, M., Mouton, S., Simanov, D., Beltman, F., Grelling, M., de Mulder, K., Arindrarto, W., Weissert, P.M., van der Elst, S., Berezikov, E., 2016. Transcriptional signatures of somatic neoblasts and germline cells in *Macrostomum lignano*. Elife 5.
Hwang, B., An, Y., Agata, K., Umesono, Y., 2015. Two distinct roles of the yorkie/yap gene during homeostasis in the planarian *Dugesia japonica*. Dev. Growth Differ. 57, 209–217.
Imai, K.S., Levine, M., Satoh, N., Satou, Y., 2006. Regulatory blueprint for a chordate

embryo. Science 312, 1183–1187.
Ishida, S., 1989. Further studies on the shell-forming granules and eggshell formation in polyclads (Turbellaria, Platyhelminthes). Sci. Rep. Hirosaki Univ. 36, 55–72.
Ishida, S.T., W., 1986. Eggshell formation in polyclads (turbellaria). Hydrobiologia 132, 127–135.
Janicke, T., Marie-Orleach, L., De Mulder, K., Berezikov, E., Ladurner, P., Vizoso, D.B., Scharer, L., 2013. Sex allocation adjustment to mating group size in a simultaneous hermaphrodite. Evolution 67, 3233–3242.
Kuales, G., De Mulder, K., Glashauser, J., Salvenmoser, W., Takashima, S., Hartenstein, V., Berezikov, E., Salzburger, W., Ladurner, P., 2011. Boule-like genes regulate male and female gametogenesis in the flatworm *Macrostomum lignano*. Dev. Biol. 357, 117–132.
Kudoh, T., Tsang, M., Hukriede, N.A., Chen, X., Dedekian, M., Clarke, C.J., Kiang, A., Schultz, S., Epstein, J.A., Toyama, R., Dawid, I.B., 2001. A gene expression screen in zebrafish embryogenesis. Genome Res. 11, 1979–1987.
Ladurner, P., Rieger, R., Baguna, J., 2000. Spatial distribution and differentiation potential of stem cells in hatchlings and adults in the marine platyhelminth *Macrostomum sp.*: a bromodeoxyuridine analysis. Dev. Biol. 226, 231–241.
Ladurner, P., Pfister, D., Seifarth, C., Schärer, L., Mahlknecht, M., Salvenmoser, W., Gerth, R., Marx, F., Rieger, R., 2005a. Production and characterisation of cell- and tissue-specific monoclonal antibodies for the flatworm *Macrostomum sp*. Histochem. Cell Biol. 123, 89–104.
Ladurner, P., Schärer, L., Salvenmoser, W., Rieger, R.M., 2005b. A new model organism among the lower Bilateria and the use of digital microscopy in taxonomy of meiobenthic platyhelminthes: *Macrostomum lignano*, n. sp. (Rhabditophora, Macrostomorpha). J. Zool. Syst. Evol. Res. 43, 114–126.
Langmead, B., Salzberg, S.L., 2012. Fast gapped-read alignment with Bowtie 2. Nat. Methods 9, 357–359.
Lapan, S.W., Reddien, P.W., 2011. dlx and sp6-9 Control optic cup regeneration in a prototypic eye. PLoS Genet. 7, e1002226.
Lapan, S.W., Reddien, P.W., 2012. Transcriptome analysis of the planarian eye identifies ovo as a specific regulator of eye regeneration. Cell Rep. 2, 294–307.
Laumer, C.E., Hejnol, A., Giribet, G., 2015. Nuclear genomic signals of the 'microturbellarian' roots of platyhelminth evolutionary innovation. Elife 4.
Lein, E.S., Hawrylycz, M.J., Ao, N., Ayres, M., Bensinger, A., Bernard, A., Boe, A.F., Boguski, M.S., Brockway, K.S., Byrnes, E.J., Chen, L., Chen, L., Chen, T.M., Chin, M.C., Chong, J., Crook, B.E., Czaplinska, A., Dang, C.N., Datta, S., Dee, N.R., Desaki, A.L., Desta, T., Diep, E., Dolbeare, T.A., Donelan, M.J., Dong, H.W., Dougherty, J.G., Duncan, B.J., Ebbert, A.J., Eichele, G., Estin, L.K., Faber, C., Facer, B.A., Fields, R., Fischer, S.R., Fliss, T.P., Frensley, C., Gates, S.N., Glattfelder, K.J., Halverson, K.R., Hart, M.R., Hohmann, J.G., Howell, M.P., Jeung, D.P., Johnson, R.A., Karr, P.T., Kawal, R., Kidney, J.M., Knapik, R.H., Kuan, C.L., Lake, J.H., Laramee, A.R., Larsen, K.D., Lau, C., Lemon, T.A., Liang, A.J., Liu, Y., Luong, L.T., Michaels, J., Morgan, J.J., Morgan, R.J., Mortrud, M.T., Mosqueda, N.F., Ng, L.L., Ng, R., Orta, G.J., Overly, C.C., Pak, T.H., Parry, S.E., Pathak, S.D., Pearson, O.C., Puchalski, R.B., Riley, Z.L., Rockett, H.R., Rowland, S.A., Royall, J.J., Ruiz, M.J., Sarno, N.R., Schaffnit, K., Shapovalova, N.V., Sivisay, T., Slaughterbeck, C.R., Smith, S.C., Smith, K.A., Smith, B.I., Sodt, A.J., Stewart, N.N., Stumpf, K.R., Sunkin, S.M., Sutram, M., Tam, A., Teemer, C.D., Thaller, C., Thompson, C.L., Varnam, L.R., Visel, A., Whitlock, R.M., Wohnoutka, P.E., Wolkey, C.K., Wong, V.Y., Wood, M., Yaylaoglu, M.B., Young, R.C., Youngstrom, B.L., Yuan, X.F., Zhang, B., Zwingman, T.A., Jones, A.R., 2007. Genome-wide atlas of gene expression in the adult mouse brain. Nature 445, 168–176.
Lengerer, B., Pjeta, R., Wunderer, J., Rodrigues, M., Arbore, R., Schärer, L., Berezikov, E., Hess, M.W., Pfaller, K., Egger, B., Obwegeser, S., Salvenmoser, W., Ladurner, P., 2014. Biological adhesion of the flatworm *Macrostomum lignano* relies on a duo-gland system and is mediated by a cell type-specific intermediate filament protein. Front. Zool. 11, 12.
Lengerer, B., Hennebert, E., Flammang, P., Salvenmoser, W., Ladurner, P., 2016. Adhesive organ regeneration in *Macrostomum lignano*. BMC Dev. Biol. 16.
LoCascio, S.A., Lapan, S.W., Reddien, P.W., 2017. Eye absence does not regulate planarian stem cells during eye regeneration. Dev. Cell 40, 381–391, (e383).
Love, M.I., Huber, W., Anders, S., 2014. Moderated estimation of fold change and dispersion for RNA-seq data with DESeq. 2. Genome Biol. 15, 550.
Miwata, K., Chiba, T., Horii, R., Yamada, L., Kubo, A., Miyamura, D., Satoh, N., Satou, Y., 2006. Systematic analysis of embryonic expression profiles of zinc finger genes in Ciona intestinalis. Dev. Biol. 292, 546–554.
Molnar, C., Casado, M., Lopez-Varea, A., Cruz, C., de Celis, J.F., 2012. Genetic annotation of gain-of-function screens using RNA interference and in situ hybridization of candidate genes in the Drosophila wing. Genetics 192, 741–752.
Morgan, T.H., 1901. Growth and regeneration in *Planaria lugubris*. Arch. Entwickl. Org. 13, 179–212.
Morris, J., Cardona, A., De Miguel-Bonet Mdel, M., Hartenstein, V., 2007. Neurobiology of the basal platyhelminth *Macrostomum lignano*: map and digital 3D model of the juvenile brain neuropile. Dev. Genes Evol. 217, 569–584.
Neidhardt, L., Gasca, S., Wertz, K., Obermayr, F., Worpenberg, S., Lehrach, H., Herrmann, B.G., 2000. Large-scale screen for genes controlling mammalian embryogenesis, using high-throughput gene expression analysis in mouse embryos. Mech. Dev. 98, 77–94.
Nimeth, K., Ladurner, P., Gschwentner, R., Salvenmoser, W., Rieger, R., 2002. Cell renewal and apoptosis in *Macrostomum sp*. [Lignano]. Cell Biol. Int. 26, 801–815.
Nimeth, K.T., Egger, B., Rieger, R., Salvenmoser, W., Peter, R., Gschwentner, R., 2007. Regeneration in *Macrostomum lignano* (Platyhelminthes): cellular dynamics in the neoblast stem cell system. Cell Tissue Res. 327, 637–646.
Pang, Q., Gao, L., Hu, W., An, Y., Deng, H., Zhang, Y., Sun, X., Zhu, G., Liu, B., Zhao, B., 2016. De novo transcriptome analysis provides insights into immune related genes and the RIG-I-Like receptor signaling pathway in the freshwater planarian (Dugesia japonica). PLoS One 11, e0151597.
Pfister, D., De Mulder, K., Philipp, I., Kuales, G., Hrouda, M., Eichberger, P., Borgonie, G., Hartenstein, V., Ladurner, P., 2007. The exceptional stem cell system of *Macrostomum lignano*: screening for gene expression and studying cell proliferation by hydroxyurea treatment and irradiation. Front. Zool. 4, 9.
Pfister, D., De Mulder, K., Hartenstein, V., Kuales, G., Borgonie, G., Marx, F., Morris, J., Ladurner, P., 2008. Flatworm stem cells and the germ line: developmental and evolutionary implications of macvasa expression in *Macrostomum lignano*. Dev. Biol. 319, 146–159.
Pollet, N., Niehrs, C., 2001. Expression profiling by systematic high-throughput in situ hybridization to whole-mount embryos. Methods Mol. Biol. 175, 309–321.
Pollet, N., Muncke, N., Verbeek, B., Li, Y., Fenger, U., Delius, H., Niehrs, C., 2005. An atlas of differential gene expression during early Xenopus embryogenesis. Mech. Dev. 122, 365–439.
Ramm, S.A., Lengerer, B., Arbore, R., Pjeta, R., Wunderer, J., Giannakara, A., Berezikov, E., Ladurner, P., Schärer, L., The Transcriptional Landscape of Sex Allocation Plasticity: Socially-Sensitive Gene Expression in the Hermaphroditic Flatworm *Macrostomum lignano*. Unpublished results.
Reddien, P.W., 2013. Specialized progenitors and regeneration. Development 140, 951–957.
Reddien, P.W., Sanchez Alvarado, A., 2004. Fundamentals of planarian regeneration. Annu. Rev. Cell Dev. Biol. 20, 725–757.
Rink, J.C., 2013. Stem cell systems and regeneration in planaria. Dev. Genes Evol. 223, 67–84.
Rink, J.C., Vu, H.T., Sanchez Alvarado, A., 2011. The maintenance and regeneration of the planarian excretory system are regulated by EGFR signaling. Development 138, 3769–3780.
Roberts-Galbraith, R.H., Newmark, P.A., 2015. On the organ trail: insights into organ regeneration in the planarian. Curr. Opin. Genet. Dev. 32, 37–46.
Roberts-Galbraith, R.H., Brubacher, J.L., Newmark, P.A., 2016. A functional genomics screen in planarians reveals regulators of whole-brain regeneration. Elife 5.
Rofatto, H.K., Parker-Manuel, S.J., Barbosa, T.C., Tararam, C.A., Alan Wilson, R., Leite, L.C., Farias, L.P., 2012. Tissue expression patterns of *Schistosoma mansoni* venom allergen-like proteins 6 and 7. Int. J. Parasitol. 42, 613–620.
Sanchez Alvarado, A., Newmark, P.A., Robb, S.M., Juste, R., 2002. The *Schmidtea mediterranea* database as a molecular resource for studying platyhelminthes, stem cells and regeneration. Development 129, 5659–5665.
Schärer, L., 2009. Tests of sex allocation theory in simultaneously hermaphroditic animals. Evolution 63, 1377–1405.
Schärer, L., Ladurner, P., 2003. Phenotypically plastic adjustment of sex allocation in a simultaneous hermaphrodite. Proc. Biol. Sci. 270, 935–941.
Schärer, L., Vizoso, D.B., 2007. Phenotypic plasticity in sperm production rate: there's more to it than testis size. Evol. Ecol. 21, 295–306.
Scimone, M.L., Srivastava, M., Bell, G.W., Reddien, P.W., 2011. A regulatory program for excretory system regeneration in planarians. Development 138, 4387–4398.
Sekii, K., Salvenmoser, W., De Mulder, K., Schärer, L., Ladurner, P., 2009. Melav2, an elav-like gene, is essential for spermatid differentiation in the flatworm *Macrostomum lignano*. BMC Dev. Biol. 9, 62.
Shekhar, S., Pernier, J., Carlier, M.F., 2016. Regulators of actin filament barbed ends at a glance. J. Cell Sci. 129, 1085–1091.
Shibata, N., Hayashi, T., Fukumura, R., Fujii, J., Kudome-Takamatsu, T., Nishimura, O., Sano, S., Son, F., Suzuki, N., Araki, R., Abe, M., Agata, K., 2012. Comprehensive gene expression analyses in pluripotent stem cells of a planarian, *Dugesia japonica*. Int. J. Dev. Biol. 56, 93–102.
Simanov, D., 2014. Genomic Resources for the flAtworm Model Organism *Macrostomum lignano*, Hubrecht Institute of The Royal Acedemy of Arts and Sciences. University Medical Center Utrecht.
Thi-Kim Vu, H., Rink, J.C., McKinney, S.A., McClain, M., Lakshmanaperumal, N., Alexander, R., Sanchez Alvarado, A., 2015. Stem cells and fluid flow drive cyst formation in an invertebrate excretory organ. Elife 4.
Thisse, C., Thisse, B., 2008. High-resolution in situ hybridization to whole-mount zebrafish embryos. Nat. Protoc. 3, 59–69.
Tomancak, P., Beaton, A., Weiszmann, R., Kwan, E., Shu, S., Lewis, S.E., Richards, S., Ashburner, M., Hartenstein, V., Celniker, S.E., Rubin, G.M., 2002. Systematic determination of patterns of gene expression during Drosophila embryogenesis. Genome Biol. 3, (RESEARCH0088).
Tyler, S., 1976. Comparative ultrastructure of adhesive systems in the turbellaria. Zoomorphology 84, 1–76.
Untergasser, A., Cutcutache, I., Koressaar, T., Ye, J., Faircloth, B.C., Remm, M., Rozen, S.G., 2012. Primer3–new capabilities and interfaces. Nucleic Acids Res. 40, e115.
Verdoodt, F., Bert, W., Couvreur, M., De Mulder, K., Willems, M., 2012. Proliferative response of the stem cell system during regeneration of the rostrum in *Macrostomum lignano* (Platyhelminthes). Cell Tissue Res. 347, 397–406.
Wang, I.E., Lapan, S.W., Scimone, M.L., Clandinin, T.R., Reddien, P.W., 2016. Hedgehog signaling regulates gene expression in planarian glia. Elife 5.
Wang, J., Collins, J.J., 3rd, 2016. Identification of new markers for the *Schistosoma mansoni* vitelline lineage. Int. J. Parasitol. 46, 405–410.
Wasik, K., Gurtowski, J., Zhou, X., Ramos, O.M., Delas, M.J., Battistoni, G., El Demerdash, O., Falciatori, I., Vizoso, D.B., Smith, A.D., Ladurner, P., Scharer, L., McCombie, W.R., Hannon, G.J., Schatz, M., 2015. Genome and transcriptome of the regeneration-competent flatworm, *Macrostomum lignano*. Proc. Natl. Acad. Sci. USA 112, 12462–12467.
Weber, M., Wunderer, J., Lengerer, B., Pjeta, R., Rodrigues, M., Schärer, L., Ladurner, P., Ramm, S., A Targeted *In Situ* Hybridization Screen Identifies Putative Seminal Fluid Proteins in a Simultaneously Hermaphroditic Flatworm. Unpublished results.

Weiszmann, R., Hammonds, A.S., Celniker, S.E., 2009. Determination of gene expression patterns using high-throughput RNA in situ hybridization to whole-mount Drosophila embryos. Nat. Protoc. 4, 605–618.
Wilson, R.A., Li, X.H., MacDonald, S., Neves, L.X., Vitoriano-Souza, J., Leite, L.C., Farias, L.P., James, S., Ashton, P.D., DeMarco, R., Castro Borges, W., 2015. The schistosome esophagus is a 'hotspot' for microexon and lysosomal hydrolase gene expression: implications for blood processing. PLoS Negl. Trop. Dis. 9, e0004272.
Wudarski, J., Simanov, D., Ustyantsev, K., de Mulder, K., Grelling, M., Grudniewska, M., Beltman, F., Glazenburg, L., Demircan, T., Wunderer, J., Qi, W., Vizoso, D.B., Weissert, P.M., Olivieri, D., Mouton, S., Guryev, V., Aboobaker, A., Scharer, L., Ladurner, P., Berezikov, E., 2017. A platform for efficient transgenesis in Macrostomum lignano, a flatworm model organism for stem cell research. bioRxiv.
Zadesenets, K.S., Vizoso, D.B., Schlatter, A., Konopatskaia, I.D., Berezikov, E., Scharer, L., Rubtsov, N.B., 2016. Evidence for karyotype polymorphism in the free-living flatworm, *Macrostomum lignano*, a model organism for evolutionary and developmental biology. PLoS One 11, e0164915.